



Photocatalytic Removal of Antibiotics on g-C₃N₄ Using Amorphous CuO as Cocatalysts

Yue Zhao^{1,2}, Amir Zada³, Yang Yang⁴, Jing Pan², Yan Wang⁵, Zhaoxiong Yan^{1*}, Zhihua Xu^{1*} and Kezhen Qi^{1,5*}

¹Key Laboratory of Optoelectronic Chemical Materials and Devices of Ministry of Education, and Hubei Key Laboratory of Industrial Fume and Pollution Control, Jiangnan University, Wuhan, China, ²College of Life Science, Shenyang Normal University, Shenyang, China, ³Department of Chemistry, Abdul Wali Khan University Mardan, Mardan, Pakistan, ⁴College of Physical Science and Technology, Shenyang Normal University, Shenyang, China, ⁵Institute of Catalysis for Energy and Environment, College of Chemistry and Chemical Engineering, Shenyang Normal University, Shenyang, China

Amorphous CuO is considered as an excellent cocatalyst, owing to its large surface area and superior conductivity compared with its crystalline counterpart. The current work demonstrates a facile method to prepare amorphous CuO, which is grown on the surface of graphitic carbon nitride (g-C₃N₄) and is then applied for the photocatalytic degradation of tetracycline hydrochloride. The prepared CuO/g-C₃N₄ composite shows higher photocatalytic activities compared with bare g-C₃N₄. Efficient charge transfer between g-C₃N₄ and CuO is confirmed by the photocurrent response spectra and photoluminescence spectra. This work provides a facile approach to prepare low-cost composites for the photocatalytic degradation of antibiotics to safeguard the environment.

Keywords: amorphous CuO, cocatalysts, photocatalytic degradation, tetracycline hydrochloride, g-C₃N₄

OPEN ACCESS

Edited by:

Tingjiang Yan,
Qufu Normal University, China

Reviewed by:

Xiufang Chen,
Zhejiang Sci-Tech University, China
Deli Jiang,
Jiangsu University, China

*Correspondence:

Zhaoxiong Yan
zhaoxiongyan75@163.com
Zhihua Xu
xuzhihua78@sina.com
Kezhen Qi
qkzh2003@aliyun.com

Specialty section:

This article was submitted to
Catalysis and Photocatalysis,
a section of the journal
Frontiers in Chemistry

Received: 19 October 2021

Accepted: 01 November 2021

Published: 08 December 2021

Citation:

Zhao Y, Zada A, Yang Y, Pan J,
Wang Y, Yan Z, Xu Z and Qi K (2021)
Photocatalytic Removal of Antibiotics
on g-C₃N₄ Using Amorphous CuO
as Cocatalysts.
Front. Chem. 9:797738.
doi: 10.3389/fchem.2021.797738

INTRODUCTION

The release of a great deal of different refractory antibiotics applied for the diseases of animal therapy, as well as for crop production into the natural water bodies by municipal and pharmaceutical industries, is considered to be a concerning issue over the past few years. The incomplete metabolism of antibiotics results in the excessive accumulation of these compounds in the ground and on the surface of water bodies to cause strong drug toxicity and reduces the efficiency of life-saving medicines. Their long persistence in ground water has led to the generation of serious antibiotic-resistant microbiota, which is a major threat to human existence. Therefore, it is extremely important to dispose these antibiotics from the bodies of ground water before they cause severe damage to human beings and aquatic animals.

Traditional methods used for removing pollutants and antibiotics are no longer effective to ensure the safety of water. Photocatalysis (Yan et al., 2020a; Yan et al., 2020b; Zhang H. et al., 2021; Li et al., 2021; Zhu et al., 2021), a green technology has recently shown exceptional performance in the photodegradation of a large number of organic pollutants (Khaledian et al., 2019; Liu et al., 2019; Yan et al., 2019; Gholami et al., 2020; Zhang et al., 2020). As a polymeric semiconductor photocatalyst, graphitic carbon nitride (g-C₃N₄) has shown outstanding performance and is widely favored due to its low toxicity, high chemical and thermal stability, and low-cost precursor materials (Wen et al., 2017a; Qi et al., 2020b; Di et al., 2020; Shi et al., 2020; Wu et al., 2020). Its moderate band gap and suitable conduction band (CB) and valence band (VB) positions are extremely important to produce highly active reactive oxygen species (ROS) under solar light irradiation for the effective removal of

antibiotics from water (Zada et al., 2020). However, its low utilization of sunlight and high charge recombination characteristics are responsible for its low photocatalytic activity and low removal efficiency of organic pollutants (Hao et al., 2020; Wang et al., 2021). It is urgently needed to introduce the photocatalysts with improved photocatalytic activity to address water pollution.

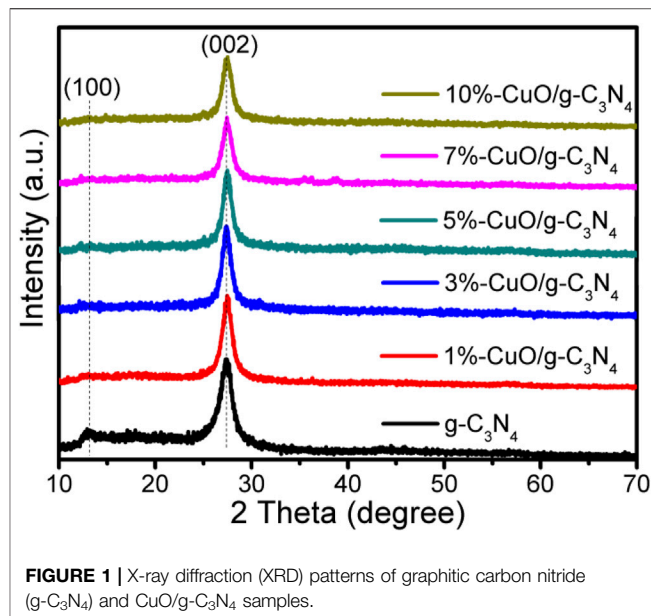
Transition metal oxides are extremely promising materials for semiconductor photocatalysts (Zhang G. et al., 2021; Shan et al., 2021). Especially, CuO is very important due to its high abundance, low cost, non-toxic property, high intrinsic thermal safety, and environmental benignity. CuO is a p-type semiconductor with a narrow band gap between 1.2 and 1.5 eV (Liu et al., 2014). It has received much attention for its extensive applications in gas sensors, solar photovoltaics, and as a heterogeneous catalyst. It is well known that amorphous metal oxides or metal sulfides are superior to their crystalline counterparts as they possess the advantage of lower synthesis temperature, simpler synthesis process, and larger specific area. Moreover, a number of previous studies have highlighted its excellent hole/electron mobility in comparison to its crystalline counterpart, such as amorphous MoS_x, NiS, Co₃O₄, etc. (Yuan et al., 2015; Wen et al., 2017b; Yu et al., 2019). Amorphous materials are considered to possess excellent redox centers in bulk on the surface to process highly efficient photocatalysis compared with its crystalline form. Although the band gap of amorphous CuO is slightly larger than that of the crystalline CuO, its excellent charge conductivity and superior surface area play an extremely positive role in the photocatalytic processes (Huang et al., 2015). Thus, it is of much interest to fabricate composite photocatalysts with amorphous CuO as cocatalyst for improving the performance of photocatalysis.

In this work, a photocatalyst composed of amorphous CuO and g-C₃N₄ was fabricated utilizing a facile method, which involved heating melamine in a muffle furnace and then growing different mass percent ratios of amorphous CuO. The fabricated samples showed enhanced photodegradation activities for the removal of tetracycline hydrochloride antibiotics. The improved photocatalytic performance of CuO/g-C₃N₄ was attributed to the extended visible light absorption and enhanced charge separation after the growth of amorphous CuO as cocatalysts on the surface of g-C₃N₄. Finally, a possible photocatalytic mechanism was proposed based on the experimental results. This work provides an effective method for the design of a high-efficiency photocatalyst using amorphous cocatalysts.

EXPERIMENTAL SECTION

Synthesis

For the preparation of g-C₃N₄, 20 g of melamine was ground and transferred to a 100-ml crucible. The crucible was closed and heated in a muffle furnace at 520°C for 4 h at the rate of 2°C/min. The amorphous CuO with different mass percentage ratios was grown on the surface of g-C₃N₄ by dispersing 0.21 g of g-C₃N₄ in 20 ml of solvent (10 ml of ethanol and 10 ml of water) under



vigorous stirring for 30 min. A given mass of Cu(NO₃)₂·H₂O was added, and stirring continued for another 30 min. Two milliliters of ammonia was added to the mixture, and the mixture was then placed in a stainless steel autoclave at 120°C for 4 h. The naturally cooled mixture was centrifuged and washed three times with distilled water to remove any impurities. It was then dried at 80°C in an oven overnight and calcined at 200°C for 1 h. The samples were represented as X%-CuO/g-C₃N₄ where “X%” stands for the percentage of amorphous CuO in the mixture.

Characterization

The crystal structure of the fabricated samples was examined by x-ray diffraction (XRD) utilizing the Bruker D8 Advance Diffractometer with Cu-Kα radiation. The Fourier transform infrared (FT-IR) spectra were obtained utilizing the Nicolet Magna 560 spectrophotometer to investigate the functional groups. ESCALAB MKII x-ray photoelectron spectrometer with Mg-Kα radiation was employed to evaluate the chemical states of the elements, and the binding energies were calibrated with the binding energy of the adventitious carbon. Transmission electron microscopic (TEM) images of the samples were acquired with JEM-2010 apparatus. The ultraviolet-visible diffused reflectance spectra (UV-vis DRS) were measured with UV-3600, Shimadzu spectrophotometer with an integrating sphere attachment. The photoelectrochemical study was conducted with an IVIUM V13806 electrochemical workstation.

Evaluation of Photocatalytic Performance

The photocatalytic activities of the different samples were evaluated from the photodegradation of tetracycline hydrochloride antibiotics. Fifty milligrams of the given antibiotic was dissolved in 1,000 ml of water. Fifty milliliters of the respective solution was placed into a photochemical reactor made of quartz and mixed with 0.2 g photocatalyst. The mixture was first stirred in the dark for 30 min to attain adsorption/

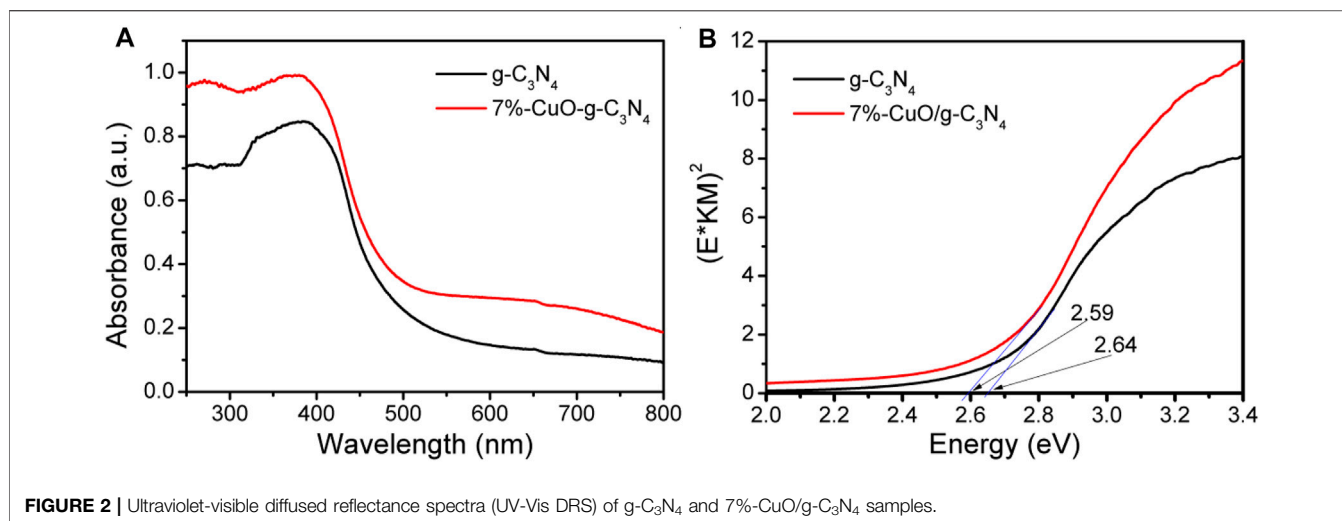


FIGURE 2 | Ultraviolet-visible diffused reflectance spectra (UV-Vis DRS) of g-C₃N₄ and 7%-CuO/g-C₃N₄ samples.

desorption equilibrium between the adsorbed and unadsorbed antibiotic molecules. It was then illuminated with a 500-W Xe lamp for 2 h at a wavelength of over 365 nm. After every interval of 20 min, 5 ml of the liquid portion was centrifuged, and the concentration of the antibiotics was examined with a UV-Vis spectrophotometer (UV-3600, Shimadzu) at 357-nm wavelength. The photoluminescence (PL) spectra were obtained by a Varian Cary Eclipse spectrometer.

RESULTS AND DISCUSSION

X-Ray Diffraction Analysis

The XRD patterns of the as-prepared samples are given in **Figure 1**. The g-C₃N₄ has two characteristic diffraction peaks, one at 13.02° and the other at 27.3°, which agrees well with the standard pattern of g-C₃N₄ (JCPDS87-1,526) (Yang et al., 2013). The peak at 13.02° is due to the inter-planar staking units of the aromatic system in conjugation, and the peak at 27.3° is due to the inter-layer structural packing units (Qi et al., 2019d; Qi et al., 2020a). These peaks are indexed to (100) and (002) crystal planes corresponding to a distance of 0.675 and 0.324 nm, respectively (Li et al., 2014; Qi et al., 2019c). After growing CuO on g-C₃N₄, no obvious peak of CuO was detected, indicating its amorphous nature. The intensity of the inter-planar staking peak of g-C₃N₄ has been reduced slightly, which shows the uniform distribution of amorphous CuO on the surface of g-C₃N₄.

Ultraviolet-Visible Diffused Reflectance Spectra Analysis

The light absorption properties of the samples were investigated by UV-Vis DRS (**Figure 2**). The g-C₃N₄ absorbs the light photons with a wavelength of 470 nm and gives a direct band gap of 2.64 eV, which is consistent with the previous report (Ong et al., 2015; Qi et al., 2021). CuO has a narrow band gap of lower than 1.5 eV, which means a strong visible light absorption ability (Verma et al., 2019). When amorphous CuO was grown on

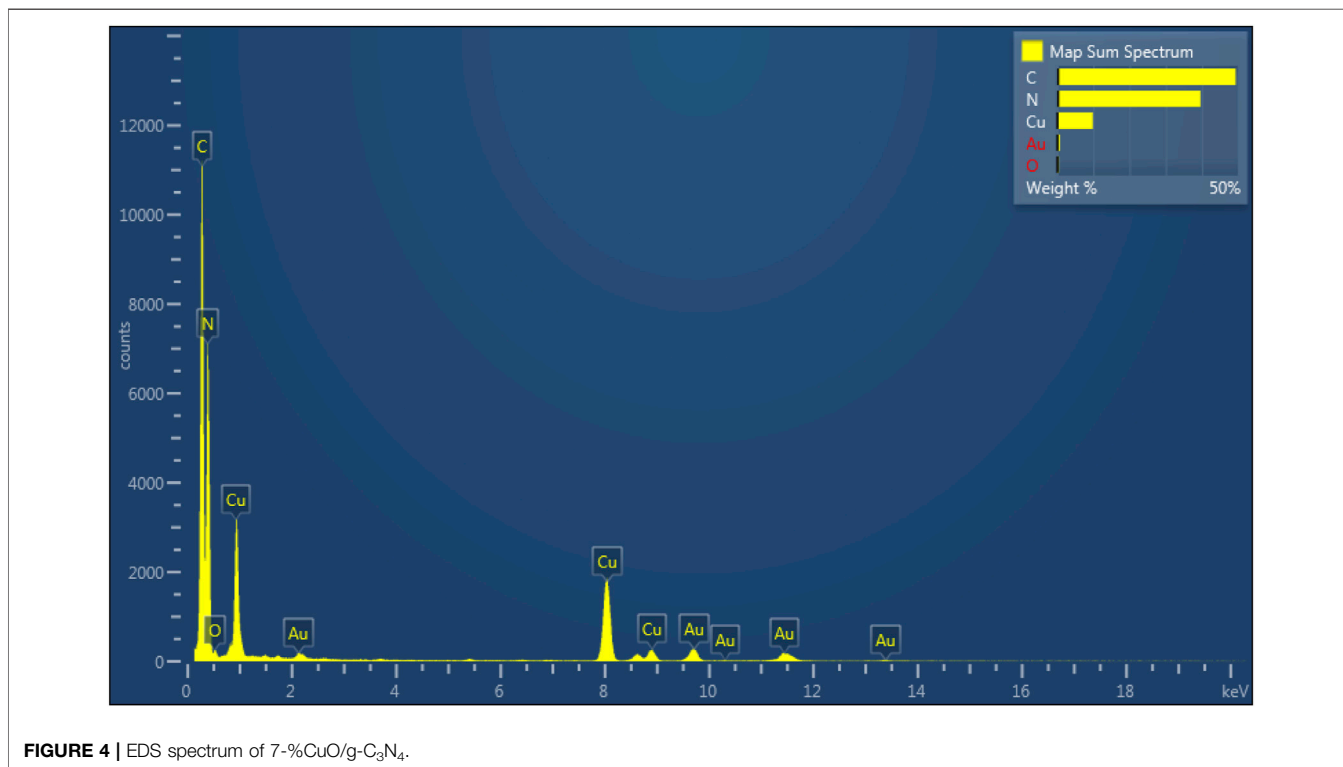
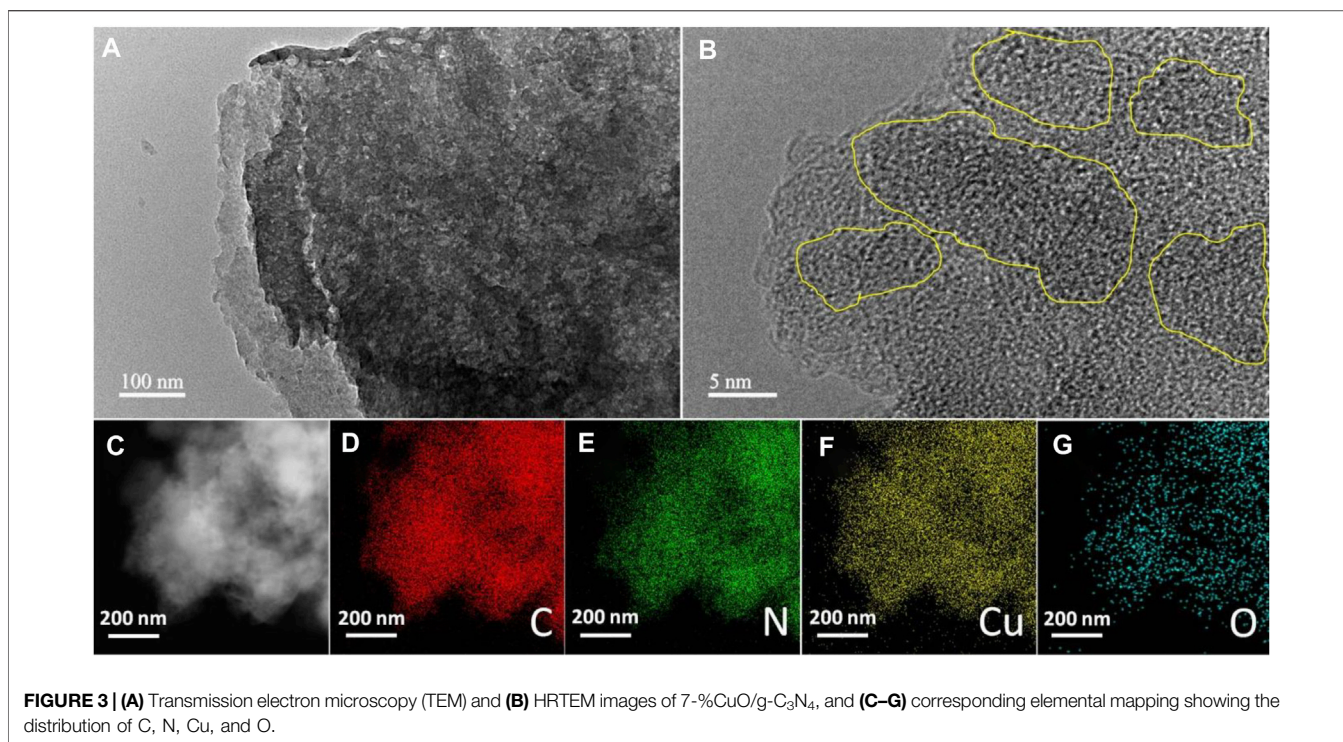
the surface of g-C₃N₄, the light absorption was slightly increased, and the absorption wavelength was shifted slightly toward the higher wavelength side. Compared with g-C₃N₄, the absorption edge of 7%-CuO/g-C₃N₄ was shifted to 479 nm at 2.59 eV. The red shift results from the mixing of the electron orbitals of CuO and g-C₃N₄. The 7%-CuO/g-C₃N₄ sample shows a broad shoulder peak ranging from 600 to 800 nm because of the d-d transition between the energy levels of Cu2p orbital (Qi et al., 2020c). The above result concludes that CuO has been successfully loaded on the surface of g-C₃N₄. The light absorption property of g-C₃N₄ has been increased after the loading of CuO. Thus, more visible light photons can be utilized by CuO/g-C₃N₄ for enhanced photoactivity.

Transmission Electron Microscopy Analysis

TEM measurement is an effective method to study the structural properties of 7%-CuO/g-C₃N₄. **Figure 3A** presents the TEM image of 7%-CuO/g-C₃N₄ with thin multilayered structures. When CuO was grown on its surface, the layered structure of g-C₃N₄ still persisted, and its morphology showed no detectable changes due to a low synthesis temperature approach (**Figure 3B**). The absence of the lattice fringes of CuO in the composite is an indication that CuO is amorphous. The elemental mapping of the sample suggests the presence of C, N, O, and Cu in the composite. The distribution of both Cu and O shows that these elements are uniformly and homogeneously grown on the surface of g-C₃N₄, as shown in **Figures 3C–G**. EDS spectrum (**Figure 4**) demonstrates that C, N, Cu, and O elements are evenly distributed on the 7%-CuO/g-C₃N₄ sample. Additionally, the existence of CuO was further verified with EDS spectra.

Fourier Transform-Infrared Analysis

The FT-IR spectra were obtained to investigate the functional groups in the fabricated samples, and the results are shown in **Figure 5**. The peak at 802 cm⁻¹ is attributed to the breathing mode of triazine rings of g-C₃N₄ (Zhu et al., 2017; Huo et al., 2019). The FT-IR peaks between 1,231 and 1,620 cm⁻¹ are accredited to the C-N stretching mode of the aromatic ring,



and these originate from C≡N stretching modes (Dai et al., 2014; Li et al., 2017). A broader peak at 3,121 cm⁻¹ is attributed to the stretching vibrational mode of the -NH group of the aromatic

ring (Cao et al., 2017; Qi et al., 2020d). These peaks are slightly reduced in their intensities when amorphous CuO was grown on g-C₃N₄. The FT-IR results indicate that the structure of g-C₃N₄

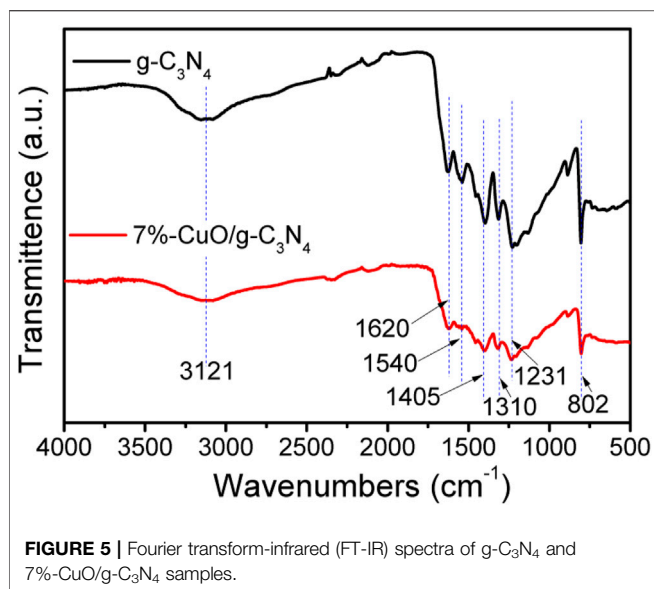


FIGURE 5 | Fourier transform-infrared (FT-IR) spectra of g-C₃N₄ and 7%-CuO/g-C₃N₄ samples.

remained unchanged after the loading of CuO. This means that CuO has been well combined with g-C₃N₄, which is consistent with the XRD result.

The surface chemical states of the elements in the composite were determined by XPS measurement. The XPS results demonstrate that the 7%-CuO/g-C₃N₄ sample contains C, N, Cu, and O elements as shown in **Figure 6A**. High-resolution XPS spectrum of carbon is shown in **Figure 6B**. Carbon shows two binding energy peaks at 284.6 and 287.6 eV, which are attributed to the sp²-hybridized C-atom bonded to the N-atom of the aromatic ring and NH₂ group, respectively (Hayat et al., 2019; Wu et al., 2015). The binding energy peaks of the N-atom are located at 398.2, 400.1, and 403.8 eV (**Figure 6C**). The former two peaks are due to the C=N-C and N-(C)₃, respectively, while the last peak is attributed to the π-π* satellite (Lin et al., 2015; Qi et al., 2019a). The binding energy peak at 932.6 eV with a satellite peak at 942.8 eV is attributed to the Cu2p_{3/2}, and the peak at 952.6 eV with a satellite peak at 962.8 eV is due to the Cu2p_{1/2} of Cu2p (**Figure 6D**) (Shen et al., 2018). The XPS peaks of the O-atom are located at 530.4, 531.3, and 532.4 eV (**Figure 6E**), which are attributed to the O-atom of the crystal lattice of CuO and O-atom of adsorbed water molecules, respectively (Qi et al., 2018). The obtained XPS data indicate that CuO has been effectively coupled with g-C₃N₄.

Photocatalytic Activity

The photocatalytic activities of the as-prepared CuO/g-C₃N₄ composites were evaluated by selecting tetracycline hydrochloride antibiotic for degradation under the irradiation from simulated solar light ($\lambda > 365$ nm). From **Figure 7A**, the photocatalytic activity of g-C₃N₄ is very low due to poor charge separation. When amorphous CuO was grown on the surface of g-C₃N₄, the photocatalytic activities were improved, and the degradation efficiency increased as the amount of CuO increased. After reaction for 60 min, the degradation of tetracycline hydrochloride is 24% for g-C₃N₄ and

55% for 7%-CuO/g-C₃N₄. The apparent reaction rate constant (*k*) is calculated in the photocatalytic degradation of tetracycline hydrochloride (**Figure 7B**). The kinetic constant of 7%-CuO/g-C₃N₄ (0.014 min⁻¹) is almost three times higher than that of g-C₃N₄ (0.005 min⁻¹). The improved photocatalytic activity is related to the extended visible light absorption and improved charge separation due to the introduction of amorphous CuO on the surface of g-C₃N₄. Another important role of CuO is acting as an oxidation cocatalyst, which promotes the separation and transport of holes and improves the oxidation ability of the photocatalyst.

Electrochemical Analysis

The measurement of transient photocurrent against time during photoelectrochemical measurement was used to study the charge separation for photocatalysis. The photocatalysts were deposited on the surface of indium-doped tin oxide glass and were used as the working electrode, while Ag/AgCl and platinum were used as the reference electrode and counter electrode, respectively. The electrolyte solution was composed of 0.1 M KCl. The greatly improved photocatalytic activity of the optimized 7%-CuO/g-C₃N₄ sample was attributed to the excellent charge separation in the given composite. The photocurrent response spectra were obtained, as shown in **Figure 8**. The 7%-CuO/g-C₃N₄ shows enhanced photocurrent compared with pure g-C₃N₄, which suggests that charge recombination has been quenched in the given sample to impart excellent photocatalytic activity. The photocurrent response spectra show that the interface of amorphous CuO and g-C₃N₄ favors the charge transfer and separation in the composite, indicating its important role in the photocatalytic process.

Photoluminescence Analysis

In order to show the enhanced charge separation in the fabricated CuO/g-C₃N₄ composite, PL spectra were obtained, as shown in **Figure 9**. As can be observed, an emission peak of g-C₃N₄ is located at 460 nm, which agrees with the previous results (Liu and Ma, 2020; Zhang M. et al., 2021). The intensity of PL peak is high in case of g-C₃N₄, which shows poor charge separation. However, when amorphous CuO was grown over g-C₃N₄, the PL intensity was significantly reduced. Since the PL peak is low, charge separation is high (Lu et al., 2017; Qi et al., 2019b). The lower PL signal shown by the 7%-CuO/g-C₃N₄ composite is due to the adsorption of amorphous CuO on g-C₃N₄ surface that extends the internal charge transformation and decreases the charge recombination between the excited e⁻ and h⁺. This has increased the lifetime of working charges to result in increased reaction time. It is concluded that the optimized composite is suitable for enhancing the photocatalytic degradation of antibiotics due to an enhanced charge separation.

Photocatalytic Mechanism

The photocatalytic degradation of antibiotics over amorphous CuO-coupled g-C₃N₄ has been discussed in detail. The charge separation and transformation are illustrated in **Figure 10**. When irradiated with light, the electrons are promoted to the CB of

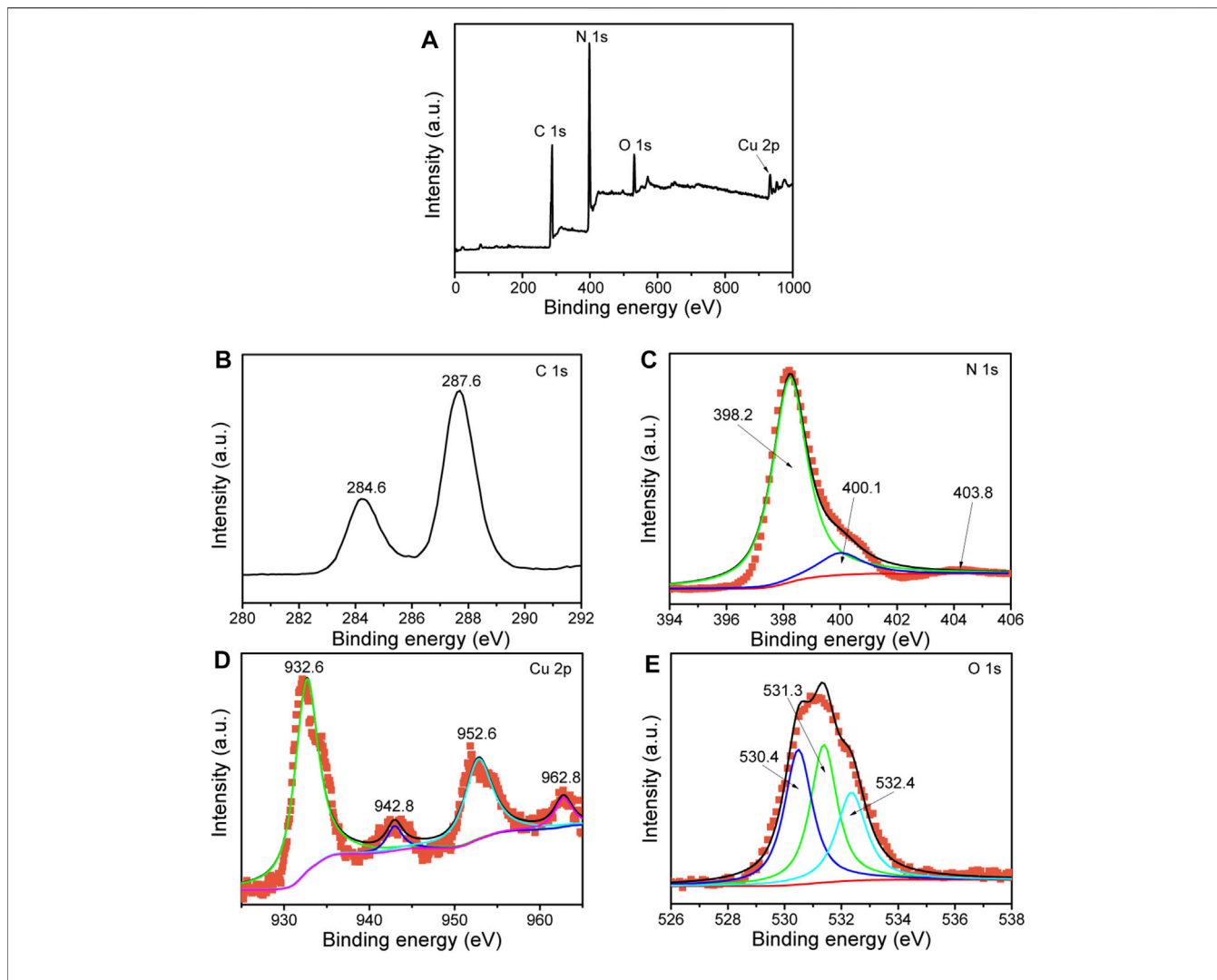


FIGURE 6 | X-ray photoelectron spectroscopy (XPS) spectra of 7%-CuO/g-C₃N₄: survey scan (A), C1s (B), N1s (C), Cu2p (D), and O1s (E).

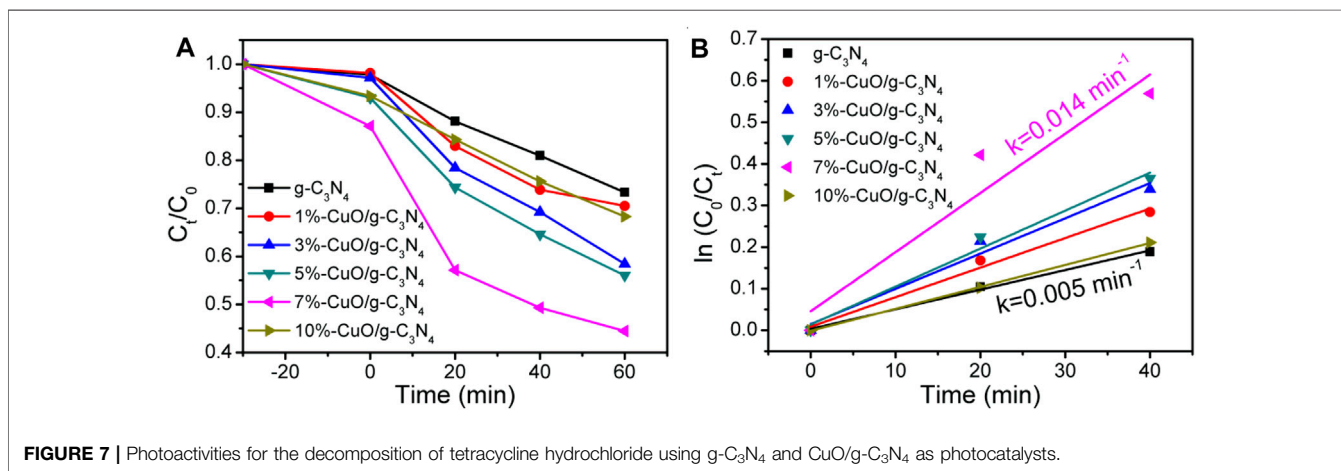


FIGURE 7 | Photoactivities for the decomposition of tetracycline hydrochloride using g-C₃N₄ and CuO/g-C₃N₄ as photocatalysts.

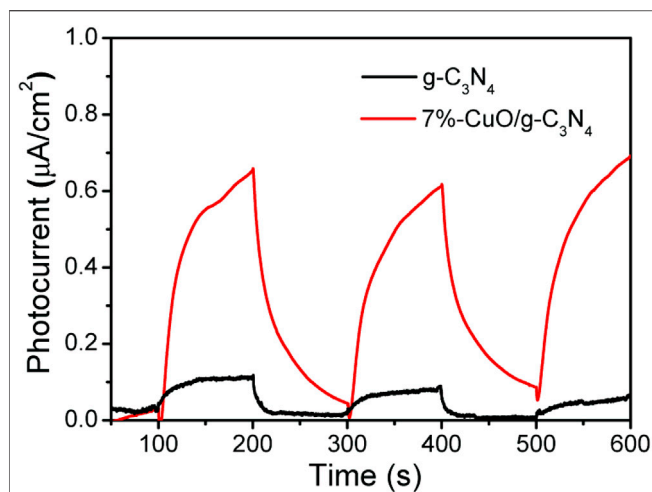


FIGURE 8 | Photocurrent response signals of 7%-CuO/g-C₃N₄.

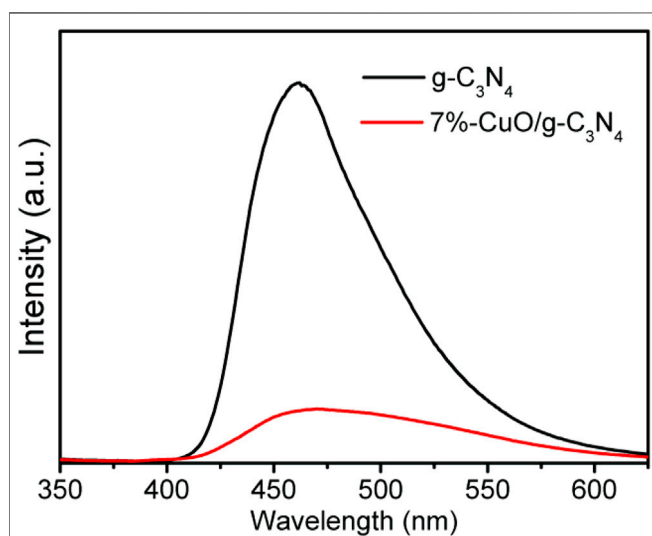


FIGURE 9 | Photoluminescence (PL) spectra of g-C₃N₄ and 7%-CuO/g-C₃N₄ samples.

g-C₃N₄, leaving positive holes in the VB. The generated electrons in the CB easily transfer to the g-C₃N₄ surface, in which the electrons can reduce the adsorbed O₂ molecules to form super oxide anions ($\cdot\text{O}_2^-$), which either directly reacts with antibiotic molecules. At the side of the VB, when p-type semiconductor CuO was closely attached on the n-type semiconductor of g-C₃N₄, the p-n junction was formed at the interface of CuO and g-C₃N₄ (Belaissa et al., 2016; Hua et al., 2019). Thus, the inner electric field in the p-n junction promotes the transfer of holes from the VB of g-C₃N₄ to CuO, and these holes oxidize the water to produce hydroxyl radicals ($\cdot\text{OH}$) to degrade the antibiotics. Thus, the CuO/g-C₃N₄ composite shows an improved photocatalytic performance for the decomposition of organic pollutants.

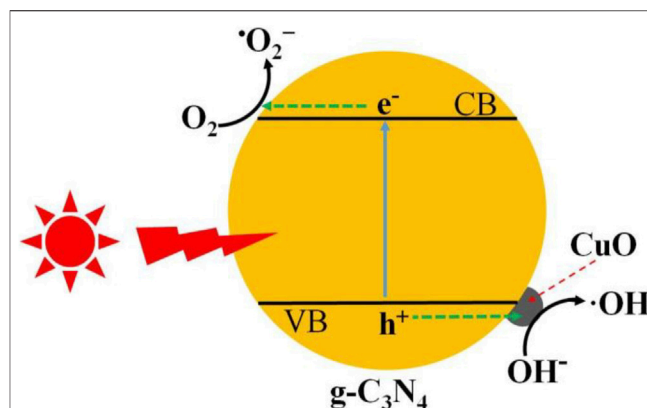


FIGURE 10 | Schematic representation of charge generation and separation in CuO/g-C₃N₄ for the degradation of tetracycline hydrochloride.

CONCLUSION

In conclusion, the amorphous CuO with excellent charge conductivity was loaded on the surface of g-C₃N₄ to form a composite and then applied for the photodegradation of tetracycline hydrochloride antibiotic. The prepared CuO/g-C₃N₄ composites show enhanced photocatalytic activities compared with the bare g-C₃N₄. It has been found that the g-C₃N₄ loaded with CuO shows the considerably positive effect for charge transfer in the composites. This work provides a facile and feasible approach for the preparation of low-cost composites for the photocatalytic degradation of antibiotics to safeguard our environment.

DATA AVAILABILITY STATEMENT

The original contributions presented in the study are included in the article/supplementary material. Further inquiries can be directed to the corresponding authors.

AUTHOR CONTRIBUTIONS

YZ conducted the catalysts preparation. AZ performed the activity test. YY, JP, and YW discussed the mechanism part. ZY, ZX, and KQ conceived the project and co-wrote the manuscript.

FUNDING

This work was supported by the Opening Project of Key Laboratory of Optoelectronic Chemical Materials and Devices of Ministry of Education, Jiangnan University (JDGD-202022), National Natural Science Foundation of China (21871111, 22075186, 21975164) and Excellent Youth Foundation of Hubei Province of China (2019CFA078). Education Office of Liaoning Province (LJKZ0997), Liaoning Revitalization Talents Program (XLYC1807238), Liaoning BaiQianWan Talents Program (2020921111).

REFERENCES

- Belaissa, Y., Nibou, D., Assadi, A. A., Bellal, B., and Trari, M. (2016). A New Hetero-junction P-CuO/N-ZnO for the Removal of Amoxicillin by Photocatalysis under Solar Irradiation. *J. Taiwan Inst. Chem. Eng.* 68, 254–265. doi:10.1016/j.jtice.2016.09.002
- Cao, S., Li, Y., Zhu, B., Jaroniec, M., and Yu, J. (2017). Facet Effect of Pd Cocatalyst on Photocatalytic CO₂ Reduction over g-C₃N₄. *J. Catal.* 349, 208–217. doi:10.1016/j.jcat.2017.02.005
- Dai, K., Lu, L., Liang, C., Liu, Q., and Zhu, G. (2014). Heterojunction of Facet Coupled g-C₃N₄/surface-Fluorinated TiO₂ Nanosheets for Organic Pollutants Degradation under Visible LED Light Irradiation. *Appl. Catal. B: Environ.* 156–157, 331–340. doi:10.1016/j.apcatb.2014.03.039
- Di, G., Zhu, Z., Dai, Q., Zhang, H., Shen, X., Qiu, Y., et al. (2020). Wavelength-dependent Effects of Carbon Quantum Dots on the Photocatalytic Activity of g-C₃N₄ Enabled by LEDs. *Chem. Eng. J.* 379, 122296. doi:10.1016/j.cej.2019.122296
- Gholami, P., Khataee, A., Cheshmeh Soltani, R. D., Dinpazhoh, R. D. C. L., and Bhatnagar, A. (2020). Photocatalytic Degradation of Gemifloxacin Antibiotic Using Zn-Co-LDH@biochar Nanocomposite. *J. Hazard. Mater.* 382, 121070. doi:10.1016/j.jhazmat.2019.121070
- Hao, S., Zhao, X., Cheng, X., Xing, Y., Ma, W., Wang, X., et al. (2020). A Mini Review of the Preparation and Photocatalytic Properties of Two-Dimensional Materials. *Front. Chem.* 8, 582146. doi:10.3389/fchem.2020.582146
- Hayat, A., Rahman, M. U., Khan, I., Khan, J., Sohail, M., Yasmeen, H., et al. (2019). Conjugated Electron Donor-Acceptor Hybrid Polymeric Carbon Nitride as a Photocatalyst for CO₂ Reduction. *Molecules* 24, 1779. doi:10.3390/molecules24091779
- Hua, S., Qu, D., An, L., Jiang, W., Wen, Y., Wang, X., et al. (2019). Highly Efficient P-type Cu₃P/n-type g-C₃N₄ Photocatalyst Through Z-Scheme Charge Transfer Route. *Appl. Catal. B: Environ.* 240, 253–261. doi:10.1016/j.apcatb.2018.09.010
- Huang, Q., Li, J., and Bi, X. (2015). The Improvement of Hole Transport Property and Optical Band gap for Amorphous Cu₂O Films. *J. Alloys Comp.* 647, 585–589. doi:10.1039/C9SE00409Bdoi:10.1016/j.jallcom.2015.06.147
- Huo, Y., Zhang, J., Dai, K., Li, Q., Lv, J., Zhu, G., et al. (2019). All-Solid-State Artificial Z-Scheme Porous g-C₃N₄/Sn₂S₃-DETA Heterostructure Photocatalyst with Enhanced Performance in Photocatalytic CO₂ Reduction. *Appl. Catal. B: Environ.* 241, 528–538. doi:10.1016/j.apcatb.2018.09.073
- Khaledian, H., Zolfaghari, P., Elhami, V., Aghbolaghy, M., Khorram, S., Karimi, A., et al. (2019). Modification of Immobilized Titanium Dioxide Nanostructures by Argon Plasma for Photocatalytic Removal of Organic Dyes. *Molecules* 24, 383. doi:10.3390/molecules24030383
- Li, W., Zhuang, C., Li, Y., Gao, C., Jiang, W., Sun, Z., et al. (2021). Anchoring Ultra-small TiO₂ Quantum Dots onto Ultra-thin and Large-Sized Mxene Nanosheets for Highly Efficient Photocatalytic Water Splitting. *Ceramics Int.* 47, 21769–21776. doi:10.1016/j.ceramint.2021.04.192
- Li, X., Zhang, X., Ma, H., Wu, D., Zhang, Y., Du, B., et al. (2014). Cathodic Electrochemiluminescence Immunosensor Based on Nanocomposites of Semiconductor Carboxylated g-C₃N₄ and Graphene for the Ultrasensitive Detection of Squamous Cell Carcinoma Antigen. *Biosens. Bioelectron.* 55, 330–336. doi:10.1016/j.bios.2013.12.039
- Li, X., Zhu, W., Lu, X., Zuo, S., Yao, C., and Ni, C. (2017). Integrated Nanostructures of CeO₂/attapulgite/g-C₃N₄ as Efficient Catalyst for Photocatalytic Desulfurization: Mechanism, Kinetics and Influencing Factors. *Chem. Eng. J.* 326, 87–98. doi:10.1016/j.cej.2017.05.131
- Lin, Q., Li, L., Liang, S., Liu, M., Bi, J., and Wu, L. (2015). Efficient Synthesis of Monolayer Carbon Nitride 2D Nanosheet with Tunable Concentration and Enhanced Visible-Light Photocatalytic Activities. *Appl. Catal. B: Environ.* 163, 135–142. doi:10.1016/j.apcatb.2014.07.053
- Liu, Q., Li, N., Qiao, Z., Li, W., Wang, L., Zhu, S., et al. (2019). The Multiple Promotion Effects of Ammonium Phosphate-Modified Ag₃PO₄ on Photocatalytic Performance. *Front. Chem.* 7, 866. doi:10.3389/fchem.2019.00866
- Liu, X., Sun, Y., Feng, C., Jin, C., and Xiao, F. (2014). Ni/amorphous CuO Core-Shell Nanocapsules with Enhanced Electrochemical Performances. *J. Power Sourc.* 245, 256–261. doi:10.1016/j.jpowsour.2013.06.136
- Liu, Y., and Ma, Z. (2020). g-C₃N₄ Modified by Meso-Tetrahydroxyphenylchlorin for Photocatalytic Hydrogen Evolution under Visible/Near-Infrared Light. *Front. Chem.* 8, 605343. doi:10.3389/fchem.2020.605343
- Lu, Z., Song, W., Ouyang, C., Wang, H., Zeng, D., and Xie, C. (2017). Enhanced Visible-Light Photocatalytic Performance of Highly-Dispersed Pt/g-C₃N₄ Nanocomposites by One-step Solvothermal Treatment. *RSC Adv.* 7, 33552–33557. doi:10.1039/C7RA04931E
- Ong, W.-J., Tan, L.-L., Chai, S.-P., Yong, S.-T., and Mohamed, A. R. (2015). Surface Charge Modification via Protonation of Graphitic Carbon Nitride (g-C₃N₄) for Electrostatic Self-Assembly Construction of 2D/2D Reduced Graphene Oxide (rGO)/g-C₃N₄ Nanostructures toward Enhanced Photocatalytic Reduction of Carbon Dioxide to Methane. *Nano Energy* 13, 757–770. doi:10.1016/j.nanoen.2015.03.014
- Qi, K., Cui, N., Zhang, M., Ma, Y., Wang, G., Zhao, Z., et al. (2021). Ionic Liquid-Assisted Synthesis of Porous boron-doped Graphitic Carbon Nitride for Photocatalytic Hydrogen Production. *Chemosphere* 272, 129953. doi:10.1016/j.chemosphere.2021.129953
- Qi, K., Li, Y., Xie, Y., Liu, S.-y., Zheng, K., Chen, Z., et al. (2019a). Ag Loading Enhanced Photocatalytic Activity of g-C₃N₄ Porous Nanosheets for Decomposition of Organic Pollutants. *Front. Chem.* 7, 91. doi:10.3389/fchem.2019.00091
- Qi, K., Liu, S.-y., and Qiu, M. (2018). Photocatalytic Performance of TiO₂ Nanocrystals With/without Oxygen Defects. *Chin. J. Catal.* 39, 867–875. doi:10.1016/S1872-2067(17)62999-1
- Qi, K., Liu, S.-y., Selvaraj, R., Wang, W., and Yan, Z. (2019b). Comparison of Pt and Ag as Co-Catalyst on g-C₃N₄ for Improving Photocatalytic Activity: Experimental and DFT Studies. *Dwt* 153, 244–252. doi:10.5004/dwt.2019.24079
- Qi, K., Liu, S.-y., Wang, R., Chen, Z., and Selvaraj, R. (2019c). Pt/g-C₃N₄ Composites for Photocatalytic H₂ Production and •OH Formation. *Dwt* 154, 312–319. doi:10.5004/dwt.2019.24068
- Qi, K., Liu, S.-y., and Zada, A. (2020a). Graphitic Carbon Nitride, A Polymer Photocatalyst. *J. Taiwan Inst. Chem. Eng.* 109, 111–123. doi:10.1016/j.jtice.2020.02.012
- Qi, K., Lv, W., Khan, I., and Liu, S.-y. (2020b). Photocatalytic H₂ Generation via CoP Quantum-Dot-Modified g-C₃N₄ Synthesized by Electroless Plating. *Chin. J. Catal.* 41, 114–121. doi:10.1016/s1872-2067(19)63459-5
- Qi, K., Xie, Y., Wang, R., Liu, S.-y., and Zhao, Z. (2019d). Electroless Plating Ni-P Cocatalyst Decorated g-C₃N₄ with Enhanced Photocatalytic Water Splitting for H₂ Generation. *Appl. Surf. Sci.* 466, 847–853. doi:10.1016/j.apsusc.2018.10.037
- Qi, K., Xing, X., Zada, A., Li, M., Wang, Q., Liu, S.-y., et al. (2020c). Transition Metal Doped ZnO Nanoparticles with Enhanced Photocatalytic and Antibacterial Performances: Experimental and DFT Studies. *Ceramics Int.* 46, 1494–1502. doi:10.1016/j.ceramint.2019.09.116
- Qi, K., Zada, A., Yang, Y., Chen, Q., and Khataee, A. (2020d). Design of 2D-2D NiO/g-C₃N₄ Heterojunction Photocatalysts for Degradation of an Emerging Pollutant. *Res. Chem. Intermed.* 46, 5281–5295. doi:10.1007/s11164-020-04262-0
- Shan, Z., Yang, Y., Shi, H., Zhu, J., Tan, X., Luan, Y., et al. (2021). Hollow Dodecahedra Graphene Oxide- Cuprous Oxide Nanocomposites with Effective Photocatalytic and Bactericidal Activity. *Front. Chem.* 9, 755836. doi:10.3389/fchem.2021.755836
- Shen, R., Xie, J., Lu, X., Chen, X., and Li, X. (2018). Bifunctional Cu₃P Decorated g-C₃N₄ Nanosheets as a Highly Active and Robust Visible-Light Photocatalyst for H₂ Production. *ACS Sust. Chem. Eng.* 6, 4026–4036. doi:10.1021/10.1021/acsschemeng.7b04403
- Shi, Z., Zhang, Y., Shen, X., Duoerkun, G., Zhu, B., Zhang, L., et al. (2020). Fabrication of g-C₃N₄/BiOBr Heterojunctions on Carbon Fibers as Weaveable Photocatalyst for Degrading Tetracycline Hydrochloride under Visible Light. *Chem. Eng. J.* 386, 124010. doi:10.1016/j.cej.2020.124010
- Verma, A., Jaithindh, D. P., and Fu, Y.-P. (2019). Photocatalytic 4-nitrophenol Degradation and Oxygen Evolution Reaction in CuO/g-C₃N₄ Composites Prepared by Deep Eutectic Solvent-Assisted Chlorine Doping. *Dalton Trans.* 48, 8594–8610. doi:10.1039/c9dt01046g
- Wang, M., Wang, M., Peng, F., Sun, X., and Han, J. (2021). Fabrication of g-C₃N₄ Nanosheets Anchored with Controllable CdS Nanoparticles for Enhanced Visible-Light Photocatalytic Performance Fabrication of g-C₃N₄ Nanosheets Anchored with Controllable CdS Nanoparticles for Enhanced Visible-Light

- Photocatalytic Performance. *Front. Chem.* 9, 746031. doi:10.3389/fchem.2021.746031
- Wen, J., Xie, J., Chen, X., and Li, X. (2017a). A Review on g-C₃N₄-Based Photocatalysts. *Appl. Surf. Sci.* 391, 72–123. doi:10.1016/j.apsusc.2016.07.030
- Wen, J., Xie, J., Zhang, H., Zhang, A., Liu, Y., Chen, X., et al. (2017b). Constructing Multifunctional Metallic Ni Interface Layers in the g-C₃N₄ Nanosheets/Amorphous NiS Heterojunctions for Efficient Photocatalytic H₂ Generation. *ACS Appl. Mater. Inter.* 9, 14031–14042. doi:10.1021/acsami.7b02701
- Wu, M., Yan, J.-M., Zhang, X.-W., Zhao, M., and Jiang, Q. (2015). Ag₂O Modified g-C₃N₄ for Highly Efficient Photocatalytic Hydrogen Generation Under Visible Light Irradiation. *J. Mater. Chem. A* 3, 15710–15714. doi:10.1039/C5TA03358F
- Wu, Z., Liang, Y., Yuan, X., Zou, D., Fang, J., Jiang, L., et al. (2020). MXene Ti₃C₂ Derived Z-Scheme Photocatalyst of Graphene Layers Anchored TiO₂/g-C₃N₄ for Visible Light Photocatalytic Degradation of Refractory Organic Pollutants. *Chem. Eng. J.* 394, 124921. doi:10.1016/j.cej.2020.124921
- Yan, T., Li, N., Wang, L., Liu, Q., Jelle, A., Wang, L., et al. (2020a). How to Make an Efficient Gas-Phase Heterogeneous CO₂ Hydrogenation Photocatalyst. *Energy Environ. Sci.* 13, 3054–3063. doi:10.1039/d0ee01124j
- Yan, T., Li, N., Wang, L., Ran, W., Duchesne, P. N., Wan, L., et al. (2020b). Bismuth Atom Tailoring of Indium Oxide Surface Frustrated Lewis Pairs Boosts Heterogeneous CO₂ Photocatalytic Hydrogenation. *Nat. Commun.* 11. doi:10.1038/s41467-020-19997-y
- Yan, T., Wang, L., Liang, Y., Makaremi, M., Wood, T. E., Dai, Y., et al. (2019). Polymorph Selection towards Photocatalytic Gaseous CO₂ Hydrogenation. *Nat. Commun.* 10. doi:10.1038/s41467-019-10524-2
- Yang, Y., Guo, Y., Liu, F., Yuan, X., Guo, Y., Zhang, S., et al. (2013). Preparation and Enhanced Visible-Light Photocatalytic Activity of Silver Deposited Graphitic Carbon Nitride Plasmonic Photocatalyst. *Appl. Catal. B: Environ.* 142–143, 828–837. doi:10.1016/j.apcatb.2013.06.026
- Yu, H., Yuan, R., Gao, D., Xu, Y., and Yu, J. (2019). Ethyl Acetate-Induced Formation of Amorphous MoS_x Nanoclusters for Improved H₂-Evolution Activity of TiO₂ Photocatalyst. *Chem. Eng. J.* 375, 121934. doi:10.1016/j.cej.2019.121934
- Yuan, J., Wen, J., Gao, Q., Chen, S., Li, J., Li, X., et al. (2015). Amorphous Co₃O₄ Modified CdS Nanorods with Enhanced Visible-Light Photocatalytic H₂-Production Activity. *Dalton Trans.* 44, 1680–1689. doi:10.1039/c4dt03197k
- Zada, A., Khan, M., Qureshi, M. N., Liu, S.-y., and Wang, R. (2020). Accelerating Photocatalytic Hydrogen Production and Pollutant Degradation by Functionalizing g-C₃N₄ with SnO₂. *Front. Chem.* 7, 941. doi:10.3389/fchem.2019.00941
- Zhang, G., Ma, Y., Liu, F., Tong, Z., Sha, J., Zhao, W., et al. (2021a). Seeded Growth of Au@Cu_xO Core-Shell Mesoporous Nanospheres and Their Photocatalytic Properties. *Front. Chem.* 9, 671220. doi:10.3389/fchem.2021.671220
- Zhang, H., Li, Y., Li, W., Zhuang, C., Gao, C., Jiang, W., et al. (2021b). Designing Large-Sized Cocatalysts for Fast Charge Separation towards Highly Efficient Visible-Light-Driven Hydrogen Evolution. *Int. J. Hydrogen Energ.* 46, 28545–28553. doi:10.1016/j.ijhydene.2021.06.134
- Zhang, M., Sun, Y., Chang, X., and Zhang, P. (2021c). Template-Free Synthesis of One-Dimensional g-C₃N₄ Chain Nanostructures for Efficient Photocatalytic Hydrogen Evolution. *Front. Chem.* 9, 652762. doi:10.3389/fchem.2021.652762
- Zhang, S., Khan, I., Qin, X., Qi, K., Liu, Y., and Bai, S. (2020). Construction of 1D Ag-AgBr/AlOOH Plasmonic Photocatalyst for Degradation of Tetracycline Hydrochloride. *Front. Chem.* 8, 117. doi:10.3389/fchem.2020.00117
- Zhu, B., Xia, P., Li, Y., Ho, W., and Yu, J. (2017). Fabrication and Photocatalytic Activity Enhanced Mechanism of Direct Z-Scheme g-C₃N₄/Ag₂WO₄ Photocatalyst. *Appl. Surf. Sci.* 391, 175–183. doi:10.1016/j.apsusc.2016.07.104
- Zhu, Y., Zhao, F., Wang, F., Zhou, B., Chen, H., Yuan, R., et al. (2021). Combined the Photocatalysis and Fenton-like Reaction to Efficiently Remove Sulfadiazine in Water Using g-C₃N₄/Ag/γ-FeOOH: Insights into the Degradation Pathway from Density Functional Theory. *Front. Chem.* 9, 742459. doi:10.3389/fchem.2021.742459

Conflict of Interest: The authors declare that the research was conducted in the absence of any commercial or financial relationships that could be construed as a potential conflict of interest.

Publisher's Note: All claims expressed in this article are solely those of the authors and do not necessarily represent those of their affiliated organizations, or those of the publisher, the editors and the reviewers. Any product that may be evaluated in this article, or claim that may be made by its manufacturer, is not guaranteed or endorsed by the publisher.

Copyright © 2021 Zhao, Zada, Yang, Pan, Wang, Yan, Xu and Qi. This is an open-access article distributed under the terms of the Creative Commons Attribution License (CC BY). The use, distribution or reproduction in other forums is permitted, provided the original author(s) and the copyright owner(s) are credited and that the original publication in this journal is cited, in accordance with accepted academic practice. No use, distribution or reproduction is permitted which does not comply with these terms.